

APPLICATIONS OF VISIBLE AND INFRARED SPECTROSCOPY TO ASTRONOMY

Marcel POPESCU¹, Mirel BIRLAN², Radu Mihai GHERASE³, Adrian Bruno SONKA⁴, Marian NAIMAN⁵, Constantin P. CRISTESCU⁶

Sunt descrise două aplicații ale spectroscopiei în studiul obiectelor de pe bolta cerească. Prelucrarea și analiza datelor pentru spectrele de emisie și spectrele de reflexie sunt exemplificate folosind observațiile la quasarul PG1634+706, respectiv observațiile la asteroidul (9147) Kourakuen.

Pentru quasarul PG1634+706 s-a obținut deplasarea Doppler spre roșu a liniilor spectrale utilizând o schemă simplă de telescop și spectrometru. Rezultatul este în concordanță cu valoarea acceptată în literatura de specialitate.

Spectrul în infraroșu apropiat obținut pentru asteroidul (9147) Kourakuen a permis clasificarea acestuia în tipul vestoizilor. Utilizând acest spectru a fost făcută o descriere a compoziției suprafeței acestui obiect. Soluția comparării cu spectrele meteoritilor a scos în evidență potrivirea spectrală cu meteoritii HED.

We describe two applications of spectroscopy to study the properties of celestial bodies. Data reduction and data analysis for emission and reflection spectra in astronomy are outlined using the spectra acquired for the quasar PG1634+706 and the asteroid (9147) Kourakuen.

For the quasar PG1634+706 we obtained the Doppler redshift of the spectral lines using a basic design of a spectrometer and a telescope. Our result is in agreement with the one accepted in the literature.

The accurate near-infrared (NIR) spectrum obtained for the asteroid (9147) Kourakuen allows to classify this object as a vestoid. A description of the surface composition for this object was obtained using this spectrum. The comparison with meteorites spectra reveals a spectral matching with HED meteorites.

Keywords: spectroscopy, astronomy, asteroid, quasar

1. Introduction

Spectroscopy is one of the most powerful scientific tools for studying nature. The study of celestial bodies using spectroscopy connects astronomy with

¹ Ph.D. Student, Department of Physics, University POLITEHNICA of Bucharest, e-mail : mpopescu@imcce.fr;

² Researcher, IMCCE – Observatoire du Paris, Mirel.Birlan@imcce.fr

³ Member of Astroclub Bucharest, radu.gherases@gmail.com

⁴ Member of Astroclub Bucharest, sonka.adrian@gmail.com

⁵ Member of Astroclub Bucharest, Marian.Naiman@cchellenic.com

⁶ Professor, University POLITEHNICA of Bucharest, e-mail : cpcris@physics.pub.ro;

fundamental physics at atomic and molecular levels. The beginning of astrophysical spectroscopy could be traced back to early nineteenth century with the discovery of dark lines in the solar spectrum by W. H. Wollaston in 1802 and J. von Fraunhofer in 1815. The dark lines at discrete wavelengths arise from absorption of energy by atoms or ions in the solar atmosphere [1].

Due to atmosphere transparency, there are two spectral windows which allow the observation of celestial bodies: the visible to near-infrared region (Fig. 1), and the radio window. The X-rays and ultraviolet wavelengths are blocked due to absorption by ozone and oxygen, while the far infrared radiation is blocked mainly due to absorption by water and carbon dioxide [2].

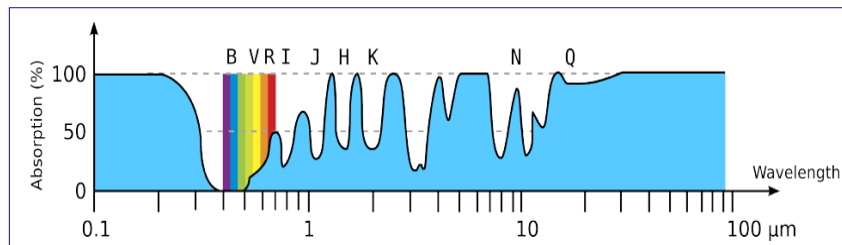


Fig. 1. Earth's atmospheric absorption as a function of wavelength (Adapted from [2])

In this article, we focus on the data reduction and data analysis for two types of spectra that we could obtain from celestial bodies: - the emission spectrum of a quasar and the reflection spectrum of an asteroid. Our observations were carried out in $0.4 - 0.7 \mu\text{m}$ and $0.8 - 2.5 \mu\text{m}$ spectral intervals.

For the emission spectroscopy, we attached a spectrometer to a telescope with the diameter of primary mirror of 200mm, with the purpose of studying the possibility to measure the redshift from quasars using this type of equipment. Thus, as application for the emission spectra, in this paper we describe the visible spectrum obtained on August 06, 2011, for PG1634+706 - a bright quasar with apparent magnitude ~ 14.7 , for which a large redshift was reported [3,4]. At this apparent magnitude, the observations with a Newtonian telescope, having a primary mirror with 200 mm diameter, are very challenging. With a robust method for data reduction we succeed to obtain a redshift ($z = 1.340$) similar with the one accepted in the scientific literature ($z = 1.337$). Both observing procedures and data reduction methods could serve as a basis for further systematic spectroscopic studies of celestial bodies using this relatively simple equipment.

In the case of reflectance spectroscopy we used the NASA InfraRed Telescope Facility (IRTF) - a 3.0 meter telescope located at the Mauna Kea Observatory, Hawaii. Reflectance spectroscopy is a remote sensing technique used to study the surfaces and atmospheres of solar system bodies. It provides

first-order information on the presence and amounts of certain ions, molecules, and minerals on the surface or in the atmosphere of the object. By looking at the changes in reflectance, the presence of absorption features can be identified. Localized dips in the spectrum indicate a particular material is absorbing light at that wavelength. From Mercury to the most distant dwarf planet, almost everything that is known about surface mineralogy has resulted from reflectance spectroscopy using ground-based telescopes [5, 6].

Our observation target for reflectance spectroscopy was the asteroid (9147) Kourakuen. Based on its colors in the visible, this asteroid was suspected to have a basaltic surface. We chose to observe the spectrum in the near-infrared (NIR) of this puzzling object from the main belt, having a favorable position and apparent magnitude (16.4) for observation with IRTF telescope on November 15, 2011.

The paper is organized as follow: in section two we present the observation methods giving also some details regarding the equipment we used. In section three we describe the data reduction and data analysis for the visible spectrum of PG1634+706. The steps for obtaining the spectrum of (9147) Kourakuen together with the analysis of the results are given in section four. The last section is dedicated to discussions and conclusions.

2. Acquiring spectra for celestial bodies

A simple way to obtain the spectra from celestial bodies is to use a prism or a transmission grating in front of a telescope objective. Depending on the equipment used, the sky quality at the observing moment and the data reduction procedures, the limiting magnitude could be pushed up to $V=15$ with a small telescope. On the other hand, a three meter telescope allows magnitudes up to $V=18$. These limiting magnitudes are valid for low resolution modes of the spectrograph.

Our first observations were carried out with telescopes having the diameter of principal mirror between 200-300 mm and a diffraction grating having 100 lines/mm. Since promising results were obtained both for stars and the quasar 3C273 we took the challenge to observe a quasar with an apparent magnitude $V=14.7$. For this run we used a *Celestron C8-NGT* telescope, which is a Newtonian type having the primary mirror of 200 mm and a focal length of 1000 mm, which means a focal ratio $f/5$. It is used on a *AS-GT (CG-5 GoTo)* equatorial mount allowing automated tracking of the objects. For image recording we used an *ATIK 314L+* CCD (charge coupled device) camera having 1.45 Megapixels (a matrix of 1391x1039), each pixel being a square - 6.45 x 6.45 μm (chip size - 8.98 x 6.71mm). This camera has a resolution of 16 bits.

The spectrum was obtained using a *Star Analyser 100* - a high efficiency *100 lines/mm* transmission diffraction grating, blazed in the first order. It was mounted in a standard *1.25 inch* diameter threaded cell which is compatible with the telescope and CCD camera. A rough calibration of the system can be estimated according to the designer formula [7] adapted to our system (Eq. 1):

$$Dispersion_{estim} [nm / pixel] = \frac{6.45}{d[cm]} \quad (1)$$

where d is the distance between grating and CCD. Our optical design allows a resolution around *1.5nm*. A precise calibration was made using known lines identified in the spectrum of a bright star.

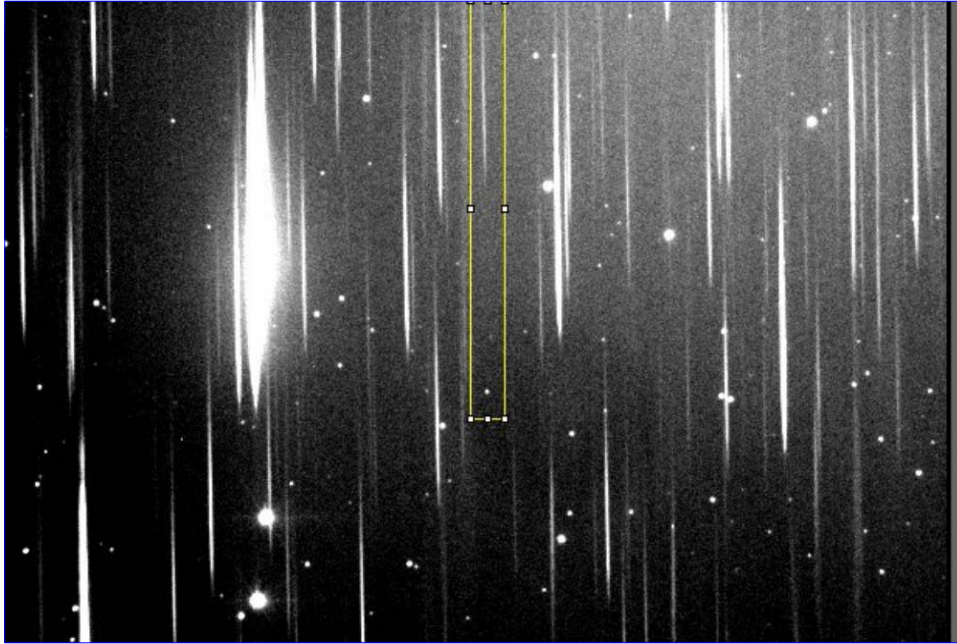


Fig. 2. Portion of the final image showing the field of quasar PG1634+706 (north is at bottom of the figure). The object and its spectrum are surrounded by a rectangle. In this image we distinguish the zero order (objects are dots) and the first order (light is dispersed)

The software used for data acquisition was Artemis Capture. The observations were carried out on 6 August 2011 in an area with low light pollution (Vălenii de Munte – Romania). The observational circumstances are given in Table 1. The final image (Fig. 2) consists in a stack of eighteen images with 90 seconds exposure time and three images with 60 seconds exposure time each, thus a 30 minutes total exposure time. Bias and flat field corrections were made using corresponding images taken at the beginning of the night.

Table 1

Observational circumstances of the selected objects: name of objects, moment of observation (UT), position of the objects (RA and DEC), visual magnitude (VMAG), airmass, and the integration time (ITIME) are presented.

Object	UT	RA[hrs]	DEC[°]	VMAG	Air mass	ITIME
PG1634+706	2011-08-05.089	16:34:29	+70:31:32	14.7	1.17	30 min
(9147) Kourakuen	2011-11-15.357	00:53:18	-04:36:21	16.4	1.14	32 min
HD4940	2011-11-15.375	00:51:17	-13:06:52	8.7	1.28	12 sec

In the last century the application of spectroscopy for astronomical objects has lead to the development of large ground-based observatories dedicated to this purpose. One of these is the NASA Infrared Telescope Facility (NASA IRTF) - a 3-meter telescope optimized for the infrared astronomy. SpeX, one of the instruments available to be used with this telescope, provides spectral resolutions of $R \sim 1000-2000$ across $0.8-2.4 \mu\text{m}$, $2.0-4.1 \mu\text{m}$, and $2.3-5.5 \mu\text{m}$, using prism cross-dispersers. Single order long slit modes are also available. A high throughput prism mode is provided for $0.8-2.5 \mu\text{m}$ spectroscopy at $R \sim 100$. It employs a 1024×1024 *Aladdin3 InSb* CCD array for acquiring the spectra. Image acquisition could be made with a 512×512 *Alladin2 CCD InSb* array [8].

Two computers manage the instrument - namely GuideDog and BigDog, the first is dedicated for pointing and tracking the object and the second is used for spectrograph setup and image acquisition. Because the asteroid (9147) Kourakuen has an apparent motion of $0.16''/\text{min}$ a differential tracking was employed.

We observed (9147) Kourakuen in the $0.8-2.5 \mu\text{m}$ spectral region with the SpeX/IRTF instrument. The observations were performed remotely from the Centre d'Observation à Distance en Astronomie à Meudon (CODAM) [9, 10] on November 15, 2011. The moment of observation (given in universal time -UT), the position of the object, the visual magnitude, the airmass (optical path length through Earth's atmosphere for light from a celestial body) and the integration time are given in Table 1. The observations were carried out using the low resolution prism mode of the spectrograph. We used a 0.8×15 arcsec slit oriented north-south.

A solar-like standard star taken at similar airmass is required to correct for atmospheric effects and to remove the signature of the Sun's spectrum in order to have only the signature of the target surface. Two G2V solar analogs were observed, namely HD22361 and HD4940. We observed the last one (HD4940) since it was at favorable airmass (the differential airmass between the asteroid and this standard star was ~ 0.14) at the moment of observation. Three pairs of images having 2 seconds exposure time for each image were sufficient to obtain a good

SNR (signal to noise ratio), considering the 8.7 magnitude of the star. When choosing the analog solar we also considered that if the star is too bright will saturate the CCD, while a fainter star will require a too long integration time.

The spectra for the asteroid and the solar analog star were obtained alternatively at two separate locations along the slit (close to top and close to bottom) following the *nodding procedure* [11].

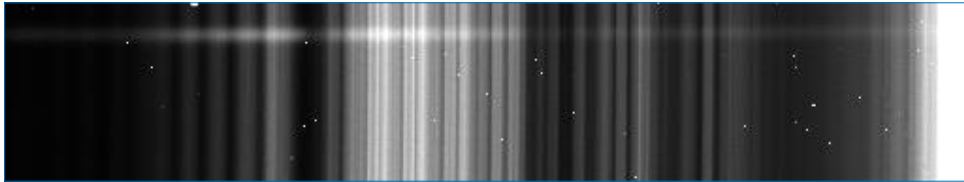


Fig. 3. Part of the image that contains the spectrum of (9147) Kourakuen. The horizontal trace represents the spectrum of the light reflected by the object.

Because the asteroid had an apparent magnitude of 16.4, eight pairs of images were taken with an exposure time of 2 minutes per image (Fig. 3). The spectrum of the object is the horizontal trace from the upper side of the image. The vertical stripes are the atmospheric lines caused by different transparency. The subtractions between adjacent images will partially remove the effect of the atmosphere (Fig. 4).

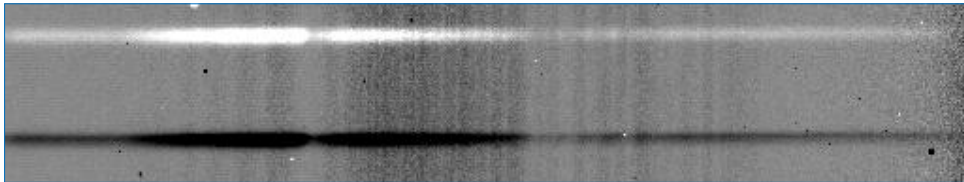


Fig. 4. Result obtained after the subtraction between two consecutive images. The white trace is the spectrum from the first image, and the dark trace (it appears black because the pixels have negative values after subtraction) is the spectrum from the second.

Preprocessing of the CCD images included bias and flat field correction. An averaged bias frame taken at the beginning of the night was used to perform bias subtraction. Flat field images were obtained using calibration lamps at the end of the night.

Our strategy was to look at objects as close to the zenith as possible, thus all observations were made at an airmass less than 1.3 (~50 deg altitude).

3. Data reduction and data analysis of emission spectra – application to the quasar PG1634 + 706

Because for these observations we did not use a lamp for wavelength calibration, this was done by identifying the position of the known lines in the star spectra. In general stellar spectra share two dominant features: the continuum - emission at all wavelengths across their spectrum and discrete absorption lines corresponding to the elements which are present in the stellar atmosphere. Hydrogen is the most common gas in the atmosphere of stars, and thus its well known absorption lines from visible ($H\alpha$, $H\beta$, $H\gamma$) can be used for wavelength calibration. Since our image (Fig. 2) contains also the spectra of some stars an accurate calibration can be made using this procedure. The value of the resolution found is given in Eq. 2:

$$Dispersion[nm / pixel] = 1.480 \pm 0.008 \quad (2)$$

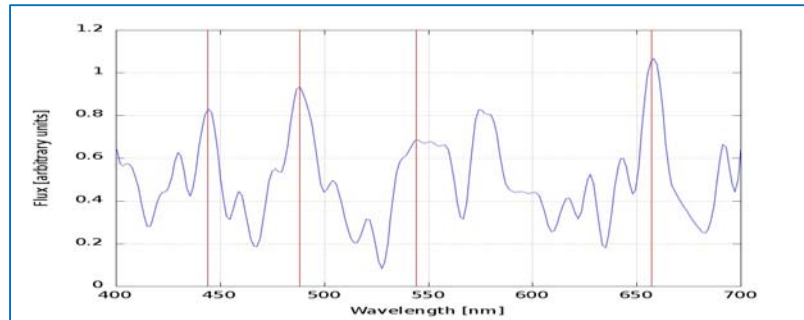


Fig. 5. PG1634 + 706 spectrum obtained after data reduction and continuum subtraction.

The preprocessing of this spectrum consists in noise reduction which was made by applying on the image a Gaussian filter with $\sigma = 2$ pixels. This filter replaces each pixel with a pixel of value proportional to a normal distribution computed over the current pixel and its neighbors [12].

The spectral profile contains a continuum part, which is the continuum emission part of the quasar modulated by the transfer function of the acquisition system (telescope, diffraction grating and CCD camera transfer functions). Continuum subtraction reduces the smoothly varying background to zero and essentially has the same effect as filtering out the long-period Fourier components of the spectra. Without continuum subtraction, the intensities of spectral lines are not clearly detectable [13]. The continuum was removed by dividing the spectrum with a fifth order polynomial curve fitting. The obtained result after data reduction and continuum subtraction is given in Fig. 5.

Quasars are objects with star-like appearance and strong radio emissions, their name being derived from *quasi-stellar radio sources*. The identification in

their spectra of the emission lines (example: hydrogen Balmer lines - $H\alpha$, $H\beta$, $H\gamma$) reveals that a large Doppler redshift exists for this type of objects. This redshift is defined as the ratio of the change in wavelength ($\Delta\lambda = \lambda_{obs} - \lambda_0$) to the non-shifted wavelength from a stationary source:

$$z = \frac{\Delta\lambda}{\lambda_0} = \sqrt{\frac{c+v}{c-v}} - 1 \quad (3)$$

where c is the speed of light and v is the recession speed of the object.

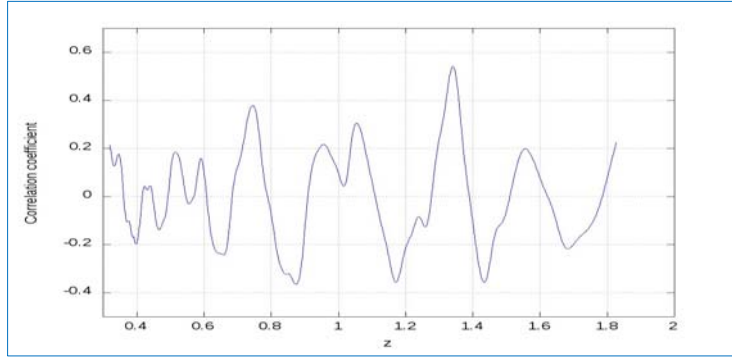


Fig 6. Correlation coefficient between quasar spectrum and the template spectrum shifted with different z .

The analysis of the obtained spectrum of the quasar PG1634+706 consists in redshift determination and application of Hubble law to determine the distance.

The most common technique [14] to determine the redshift is the cross-correlation of the observed spectrum with a template spectrum. The redshift is determined by the location of the largest peak in the cross-correlation functions. Several rest frame composite quasar spectra exist for the optical region like the one from article [15] obtained using data from Large Bright Quasar Survey (LBQS) and from article [16] based on Sloan Digital Sky Survey (SDSS). Thus for determining the redshift of our spectrum the following steps were taken: 1.) shift the template spectrum with a z varying from 0.4 to 1.8 using the step of 0.001. This is a reasonable assumption made after visual inspection of our data; 2.) at each step, the correlation coefficient between the quasar spectrum and the shifted template spectrum is computed (Fig. 6); 3.) choose the redshift corresponding to the best correlation coefficient found.

In this way, we obtained $z = 1.340$ corresponding to the peak value of the correlation coefficient equal with 0.5416. Our determination is at $\sim 3\sigma$ (where $\sigma = 0.1987$ is the standard deviation of the correlation coefficient values plotted in Fig. 6).

Considering the value found for the redshift - $z = 1.340$, the emission lines of known chemical elements could be identified in the spectrum of PG1634+706

(Table 2). Based on the emission line identification the accuracy of z determination can be ascertained: $z = 1.340 \pm 0.008$.

Table 2

Emission line identification in spectrum of PG1634 +706

Line	Rest-frame wavelength [nm]	λ shifted with $z=1.34$ [nm]	λ observed in quasar spectrum [nm]
C III]	190.6	446.0	444
Fe III	207.7	485.8	488
Fe II + CII]	232.6	544.3	544
Mg II	280.0	655.2	655

Edwin Hubble showed that there is a pattern in the speeds with which the galaxies are receding from us which implies that the Universe is expanding [15]. Observations that followed confirmed Hubble law:

$$v = H_0 \cdot d \quad (4)$$

where v is the radial velocity and d is the distance and H_0 is the Hubble constant. Recently, high-redshift measurements have been used to predict the value of H_0 [16, 17]:

$$H_0 = 70.3 \pm 1.3 \frac{km}{s \cdot Mpc} \quad (5)$$

Applying the equation (3), (4), (5) the speed of this object and the distance to it can be computed (Eq. 6).

$$v = c \cdot \frac{(z+1)^2 - 1}{(z+1)^2 + 1} = (2.073 \pm 0.018) \cdot 10^8 \frac{m}{s} \quad (6)$$

$$d = \frac{v}{H_0} = (9.644 \pm 0.16) \cdot 10^9 \text{ light years}$$

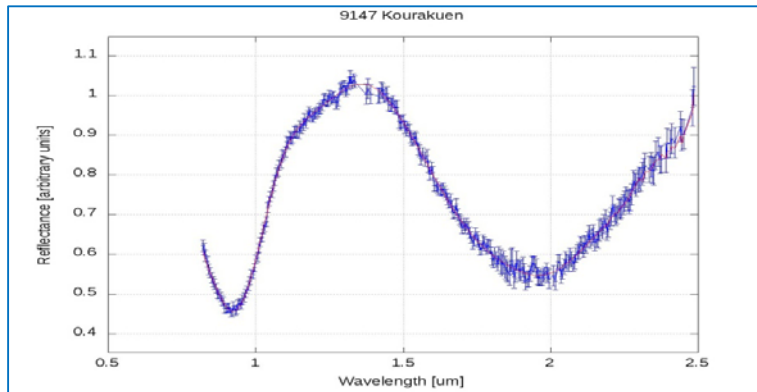
These results are in agreement with the value found by other studies of this bright quasar [3, 4, 31].

4. Data reduction and data analysis of reflection spectra – application to 9147 Kourakuen

The observation of reflection spectra from a celestial object implies additional steps in both observing method and data reduction procedure. This is due to the fact that the light reflected from the surface of the body must be divided by a spectrum of a solar-like star to determine the reflectance relative to that of the original light source, the Sun. Thus, the data reduction process for the reflection spectra consist in three steps: 1) obtain the raw spectra for the object and the solar

analog, 2) obtain the wavelength calibration of the instrument using flat field images taken with calibration lamps and 3) compute normalized reflectance spectrum by dividing the asteroid spectrum by the solar analogue spectrum and performing a correction for Earth atmospheric lines [18, 19].

Fig 7. NIR spectrum of (9147) Kourakuen.



For the first two steps, the Image Reduction and Analysis Facility (IRAF) [20] was used in conjunction with some scripts that create the command files for a specific set of IRAF instructions. For the second step, specific IDL routines were used in order to diminish the influence of the telluric bands in our spectrum and to divide the obtained spectrum by the solar analog. The obtained result for (9147) Kourakuen is given in Fig. 7.

Basaltic *asteroids* are believed to derive from bodies whose interiors reached the melting temperature of silicate rocks and subsequently differentiated [21]. (4) Vesta was the first known asteroid presenting a basaltic crust. In the last years an increasingly large number of small asteroids with a similar surface composition have been discovered [22]. (9147) Kourakuen is a main belt asteroid with an estimated diameter of 5.1 Km. Having the semi-major axis $a = 2.19 AU$, eccentricity $e = 0.108$, and inclination $i = 6^\circ.892$, this object could not belong to Vesta family considering the dynamical criteria. However, its SDSS (Sloan Digital Sky Survey) colors [23] suggests a surface composition similar to (4) Vesta (a V-type object).

The first step in analyzing the reflecting spectrum for this object consists in finding the taxonomic type of the asteroid. Taxonomic types, although not usable to determine the mineralogical compositions of the objects, help constrain mineral species that may be present on the surface of the asteroid. We used two independent methods to establish the taxonomical class of this asteroid. In a first approach, spectral data of our asteroids were compared with Bus-DeMeo taxonomic classes [24] via the MIT-SMASS on-line tool. The second approach to taxonomic classification was a procedure using a χ^2 minimization method

accounting for the mean and standard-deviation values of the Bus-DeMeo taxonomic classes [18]. Both methods lead to the same result: this object is undoubtedly a V-type (Fig. 8.a). In the Bus-DeMeo taxonomy, V-type asteroids are characterized by very strong and very narrow 1-micron absorption and strong 2-micron absorption feature [24].

Putting the spectral data obtained from telescope observations, in relation to the laboratory measurements could reveal a lot of information related to the composition of the surface of these celestial bodies. Spectroscopy of different samples made in the laboratory provides the basis upon which compositional information about unexplored or unsampled planetary surfaces is derived from remotely obtained reflectance spectra. Such a comparison could be made based on a χ^2 coefficient [11]:

$$\chi^2 = \frac{1}{N_w} \sum_i^{N_w} \frac{(R_i - f(w_i))^2}{f(w_i)} \quad (7)$$

where R_i are the reflectances obtained in laboratory, $f(w_i)$ are the object normalized reflectances and N_w is the number of points.

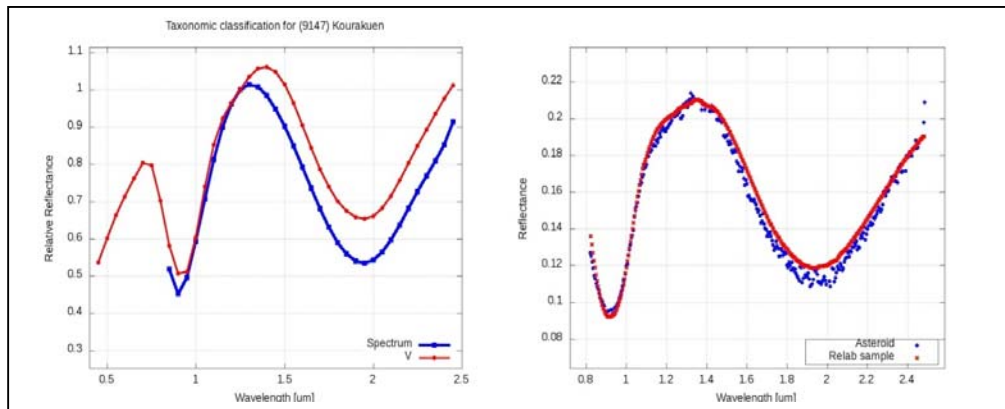


Fig 8.a) Taxonomic comparison between the polynomial fit of (9147) Kourakuen (blue) and the V-type class (red); b) Comparison between the spectrum of (9147) Kourakuen (blue) and the NIR spectrum of meteorite Pavlovka.

The Relab spectral database contains more than 15,000 spectra for different types of materials from meteorites to terrestrial rocks, man-made mixtures, and terrestrial and lunar soils [25]. We compared our spectrum with all the spectra from the Relab database, using a χ^2 minimization method and additionally, the correlation coefficient. The solution found with both methods was that the spectrum of (9147) Kourakuen is almost identical with the spectrum of Pavlovka meteorite (Fig. 8.b). The meteorite sample is of type achondrite howardite already studied so far [26, 27]. The bulk composition of the chondrules

from this meteorite contains SiO₂ (50.1%), MgO(23.7%), FeO(15%), Al₂O₃(6.2%), CaO(3.8%) [26].

Laboratory spectra similar to the spectrum of (9147) Kourakuen are those of the meteorites Roda (Achondrite Diogenite), Le Teilleul (Achondrite, Howardite) and Kapoeta (Basaltic HED Howardite). The first fifty solutions that matched our spectrum are HED (Howardite Eucrite Diogenite) meteorites. These are basaltic meteorites believed to result from large asteroids that melted to form a metallic core and basaltic magmas after the formation.

The absorption band parameters are diagnostic of the mineralogy present on the surface of the observed asteroids. The relationship between these spectral parameters and the mineralogy, particularly pyroxene and olivine, has been studied in various papers over the last years [28]. Most pyroxenes and the basaltic achondrites show a strong correlation between the position of band centers at 1 μm and 2 μm [28, 29, 30]. Thus, we computed the band minima and band centers (at 1 μm and 2 μm), defined as the wavelength position of the point of lowest reflectance before and after the removal of the continuum, respectively [28]. The computations were done using the standard procedures [31]. The results are given in Table 3.

Table 3

Band centers and band separation as deduced from Cloutis model.

BI center (μm)	BII center (μm)	Band separation [μm]
0.913 \pm 0.005	1.952 \pm 0.005	1.039 \pm 0.010

5. Discussions and conclusions

We described here two types of spectra of celestial bodies – the emission spectrum of a very far away object, the quasar PG1634 +706 and the reflection spectrum of a remnant object from the solar system formation, (9147) Kourakuen. The techniques for acquiring the spectra and the models used for data analysis are presented.

The two types of observations share common points in acquisition procedure, data reduction and data analysis methods. Conceptually the design of the acquisition system is the same: a telescope, a diffraction device (which could be a grating that works in transmission or reflection, or a prism) and the device to record the image of the spectrum – a charge coupled device (CCD). Also, extracting the spectrum from the image follows almost the same steps: the identification of the trace of the spectrum and getting pixel values, wavelength calibration, removing the Earth atmospheric influences in the spectrum. Data analysis includes the comparison between the spectra of celestial body with known spectra from the laboratory.

However the wide variety of results that can be obtained from analyzing the emission spectra and the reflection spectra from celestial bodies has led to two separate domains of astronomy.

Because PG1634 +706 is a bright quasar, it has been studied in some papers like [3, 4, 31, 32]. Our observation for this object was at the limited magnitude for the type of equipment used. With a robust method, we succeeded to extract the signal from noise and compute the redshift. Our determination of redshift $z = 1.340 \pm 0.008$, with a small telescope agrees with the value found after observation with large telescopes. The developed methods for observations and data reduction can be used as a starting point for spectroscopy of celestial bodies with small telescopes.

We obtained an accurate near-infrared spectrum of the asteroid (9147) Kourakuen. Based on this spectrum, a description of the surface composition was made. The comparisons with meteorites spectra revealed a spectral matching with HED type meteorites and in particular with the spectrum of Pavlovka meteorite. Using the Bus-DeMeo taxonomy, we classified this object as a V-type (taxonomic class describing asteroids with similar spectra as Vesta), which agrees to the type identified using a relatively more noisy spectrum by [22].

REFERENCES

- [1] *Anil K. Pradhan, Sultana N. Nahar*; Atomic Astrophysics and Spectroscopy; Cambridge University Press 2011;
- [2] *Bennoit Carry*; Etudes des proprietes physiques des asteroides par imagerie a haute resolution angulaire, Ph. D. Thesis; UNIVERSITE PARIS.DIDEROT (Paris 7), 29/09/2009
- [3] *Schmidt, M.; Green, R. F.*; Quasar evolution derived from the Palomar bright quasar survey and other complete quasar surveys; Astrophysical Journal, Part 1 (ISSN 0004-637X), vol. 269, June 15, 1983, p. 352-374.;06/1983
- [4] *Trevese, D.; et al.*; Line and continuum variability of two intermediate-redshift, high-luminosity quasars; Astronomy and Astrophysics, **Vol. 470**, Issue 2, August I 2007, pp.491-496
- [5] *Schelte John Bus*; Compositional structure in the asteroid belt: result of a spectroscopic survey; Ph. D. Thesis - MIT; 04/1999
- [6] *Francesca E. DeMeo*; La variation compositionnelle des petits corps a travers le systeme solaire; Ph. D. Thesis - Observatoire de Paris 16/06/2010
- [7] Star Analyser site: <http://www.patonhawksley.co.uk/staranalyser.html>
- [8] *Rayner, J. T.; et al* ; The Publications of the Astronomical Society of the Pacific, **Vol. 115**, Issue 805, pp. 362-382; 03/2003
- [9] *Birlan, M.; Barucci, A.; Thuillot, W.*; Solar system observations by remote observing technique: useful experience for robotic telescope strategies; Astronomische Nachrichten, **Vol.325**, Issue 6, p.571-573; 10/2004
- [10] *Birlan, M.; et al.*; Near infra-red spectroscopy of the asteroid 21 Lutetia. I. New results of long-term campaign; Astronomy and Astrophysics, **Vol. 454**, Issue 2, August I 2006, pp.677-681
- [11] *Dan Alin Nedelcu*; Modelisation Dynamique et spectroscopique des asteroides; Ph. D. Thesis - Observatoire de Paris; 23 09/2010;

- [12] Image J site: <http://imagejdocu.tudor.lu/>
- [13] *Fuqing Duan, Fuchao Wu*; Redshift Determination for Quasar Based on Similarity Measure; ICAPR 2005, LNCS 3686, pp. 529–537, 2005
- [14] *Tonry, J.; Davis, M.*; A survey of galaxy redshifts. I - Data reduction techniques; *Astronomical Journal*, **vol. 84**, Oct. 1979, p. 1511-1525; 10/1979
- [15] *Francis, Paul J.; et al.*; A high signal-to-noise ratio composite quasar spectrum; *Astrophysical Journal*, Part 1 (ISSN 0004-637X), **Vol. 373**, June 1, 1991, p. 465-470; 06/1991
- [16] *Vanden Berk, Daniel E.; et al.*; Composite Quasar Spectra from the Sloan Digital Sky Survey; *The Astronomical Journal*, **Vol. 122**, Issue 2, pp. 549-564; 08/2001
- [15] *Theo Koupeelis*; In quest of the Univers; 6th edition; Jones and Bartlett Publishers; 2011
- [16] *Komatsu, E.; et. al.*; Seven-year Wilkinson Microwave Anisotropy Probe (WMAP) Observations: Cosmological Interpretation; *The Astrophysical Journal Supplement*, **Vol.192**, Issue 2; 02/2011
- [17] *Riess, Adam G.; et al.*; A 3% Solution: Determination of the Hubble Constant with the Hubble Space Telescope and Wide Field Camera 3; *The Astrophysical Journal*, **Vol. 730**, Issue 2, article id. 119 (2011); 04/2011
- [18] *Popescu, M.; et al.*; Spectral properties of eight near-Earth asteroids; *Astronomy & Astrophysics*, **Vol. 535**, 11/2011
- [19] *Birlan, M.; Vernazza, P.; Nedelcu, D. A.*; Spectral properties of nine M-type asteroids; *Astronomy and Astrophysics*, **Vol. 475**, Issue 2, November IV 2007, pp.747-754
- [20] *Tody, Doug*; IRAF in the Nineties; *Astronomical Data Analysis Software and Systems II*, A.S.P. Conference Series, **Vol. 52**, 1993, p. 173.; 01/1993
- [21] *Gaffey, M. J.; et al.*; Mineralogy of Asteroids; *Asteroids III*, W. F. Bottke Jr., A. Cellino, P. Paolicchi, and R. P. Binzel (eds), University of Arizona Press, Tucson, p.183-204; 2002
- [22] *de Sanctis, M. C.; et al.*; Spectral and mineralogical characterization of inner main-belt V-type asteroids; *Astronomy & Astrophysics*, **Vol. 533**, 09/2011
- [23] *Nesvorný, David; et al.*; Thais, Fugitives from the Vesta family; *Icarus*, **Vol.193**, Issue 1, p. 85-95; 01/2008
- [24] *DeMeo, Francesca E.; Binzel et al.*; An extension of the Bus asteroid taxonomy into the near-infrared; *Icarus*, **Vol. 202**, Issue 1, p. 160-180.; 07/2009
- [25] Relab Spectral Database: <http://www.planetary.brown.edu/relab/>
- [26] *Olsen, Edward J.; et al.*; Chondrule-like objects and brown glasses in howardites; *Meteoritics* (ISSN 0026-1114), **vol. 25**, Sept. 1990, p. 187-194.; 09/1990
- [27] *Labotka, T. C.; Papike, J. J.*; Howardites - Samples of the regolith of the eucrite parent-body: Petrology of Frankfort, Pavlovka, Yurtuk, Malvern, and ALHA 77302; *Lunar and Planetary Science Conference*, 11th, Houston, TX, March 17-21, 1980, Proceedings. **Vol. 2.** (A82-22296 09-91) New York, Pergamon Press, 1980, p. 1103-1130.
- [28] *Cloutis, Edward A.; Gaffey, Michael J.*; Pyroxene spectroscopy revisited - Spectral-compositional correlations and relationship to geothermometry; *Journal of Geophysical Research*, **Vol. 96**, Dec. 25, 1991, p. 22,809-22,826
- [29] *Gaffey, M. J.; McCord, T. B.*; Asteroidal Surface Compositions; *Bulletin of the American Astronomical Society*, **Vol. 8**, p.459; 06/1976
- [30] *Adams, J. B.; McCord, T. B.*; The use of ground-based telescopes in determining the composition of the surfaces of solar system objects.; *Moon*, **Vol. 11**, p. 429 - 430; 12/1974
- [31] *Cloutis, Edward A.; et al.*; Calibrations of phase abundance, composition, and particle size distribution for olivine-orthopyroxene mixtures from reflectance spectra; *Journal of Geophysical Research*, **Vol. 91**, Oct. 1986, p. 11641-11653.